ELSEVIER

Ceramics International 28 (2002) 419–423

CERAMICS INTERNATIONAL

www.elsevier.com/locate/ceramint

Phase development and dielectric characteristics of the $Pb(Mg_{1/3}Ta_{2/3})O_3$-modified $Pb[(Zn_{1/3}Ta_{2/3}),(Mg_{1/3}Nb_{2/3})]O_3$ system

Min-Chul Chae, Seung-Mo Lim, Nam-Kyoung Kim*

Department of Inorganic Materials Engineering, Kyungpook National University, Taegu 702-701, South Korea

Received 9 July 2001; received in revised form 11 September 2001; accepted 15 October 2001

Abstract

The effects of $Pb(Mg_{1/3}Ta_{2/3})O_3$ substitution to a multiple-octahedral system $Pb[(Zn_{1/3}Ta_{2/3}),(Mg_{1/3}Nb_{2/3})]O_3$ on perovskite phase development and dielectric characteristics are reported. Selected composition powders of the modified system were prepared using a B-site precursor method. Development of the B-site precursor and perovskite phases were investigated by X-ray diffraction. Low-frequency weak-field dielectric properties of sintered pellets were examined. Phase transition modes reflected in the dielectric constant spectra were further analyzed in terms of diffuseness parameters.

Keywords: C. Dielectric properties; D. Perovskites; Phase developments; Diffuseness

1. Introduction

Among the complex perovskite families of $A(B',B'')O_3$, lead magnesium niobate $Pb(Mg_{1/3}Nb_{2/3})O_3$ (PMN) is a prototype relaxor ferroelectric compound possessing quite high maximum dielectric constants ($\leqslant$20,000), along with diffuse modes in the phase transition. Although it is not easy to prepare the monophasic perovskite PMN by conventional one-step calcination, the persistent formation of pyrochlore can be effectively bypassed by the so-called "columbite process" [1] or more comprehensively by the "B-site precursor method" [2]. Meanwhile, lead magnesium tantalate $Pb(Mg_{1/3}Ta_{2/3})O_3$ (PMT, tantalum-analog of PMN) is also a ferroelectric relaxor, with a maximum dielectric constant of $\leqslant$9000 [3,4]. Synthesis and dielectric properties of PMT have been widely reported [3–7].

In contrast to PMN and PMT, preparation of lead zinc niobate $Pb(Zn_{1/3}Nb_{2/3})O_3$ (PZN) of perovskite structure by solid-state reaction at atmospheric pressure turned out to be virtually impossible. Powders of the perovskite PZN can only be prepared under high pressures [8] or via novel routes of mechanochemical milling [9], whereas single crystalline forms were grown by the aid of fluxes [10,11]. However, any attempt to synthesize lead zinc tantalate $Pb(Zn_{1/3}Ta_{2/3})O_3$ (PZT, tantalum-analog of PZN) in a perovskite structure has not succeeded thus far [12–14]. It should be noted that PZT, in the present paper, does not stand for $Pb(Zr,Ti)O_3$.

It has been reported that dielectric characteristics of a $(1-x)$PZT–xPMN system are excellent (except for pyrochlore-rich compositions of $x\leqslant0.4$) in that high values of the maximum dielectric constant ($>$13,000) are attainable at -13 to -5 °C, slightly below room temperature [14]. In the present study, therefore, compositions of the PZT-PMN system were modified by the introduction of 20 mol% PMT in order to promote perovskite developments, thereby improving the dielectric properties (especially of PZT-rich compositions).

2. Experimental

Nominal compositions of the system under investigation can be expressed as 0.2PMT–$(0.8-x)$PZT–xPMN (i.e. $Pb[(Mg_{1/3}Ta_{2/3})_{0.2}(Zn_{1/3}Ta_{2/3})_{0.8-x}(Mg_{1/3}Nb_{2/3})_x]O_3$), where values of x ranged from 0.0 to 0.8 at constant intervals of 0.2. Starting materials were high-purity ($>$99.5%) chemicals of PbO, MgO, ZnO, Ta_2O_5, and Nb_2O_5. In order to maintain stoichiometries as closely

* Corresponding author. Tel.: +82-53-950-5636; fax: +82-53-950-5645.

E-mail address: nkkim@knu.ac.kr (N.-K. Kim).

0272-8842/02/$22.00
PII: S0272-8842(01)00112-2

to the nominal compositions as possible, moisture contents of the raw chemicals and of the synthesized B-site precursors were measured and introduced into the batch calculation.

Powders of the B-site precursor system $[(Mg_{1/3}Ta_{2/3})_{0.2}(Zn_{1/3}Ta_{2/3})_{0.8-x}(Mg_{1/3}Nb_{2/3})_x]O_2$ (i.e. $[Mg_{(0.2+x)/3}Zn_{(0.8-x)/3}Ta_{(2.0-2x)/3}Nb_{2x/3}]O_2$) were prepared from the raw materials by wet milling under alcohol, drying and calcinations at 1100–1200 °C for 2 h. The calcination procedures were repeated once to promote the phase developments, with intermediate steps of milling and drying. After PbO addition to the B-site precursors, the powders were reacted at 800–850 °C for 2 h, followed by milling, drying and recalcinations at 800–1000 °C for an additional 2 h. Calcined powders were checked by X-ray diffractometry (XRD, Cu$K_{\alpha 1}$) for the identification of developed structures. Perovskite yields were estimated by simple comparison between intensities of (110) and (222) reflections for the perovskite and pyrochlore structures, respectively. The powders were then isostatically pressed into pellets and fired for 1 h in a multiple-enclosure crucible setup [5] to suppress lead loss at elevated temperatures. Sintered pellets were ground/polished to attain parallel sides and bulk densities were measured geometrically. Major faces of the sample pellets were electroded by gold sputtering, and dielectric constants and losses were measured on cooling, using an impedance analyzer (10^{3-6} Hz) under weak oscillation levels of ~1 V/mm.

3. Results and discussion

Fig. 1 displays room temperature X-ray diffractograms of the B-site precursor system. At $x=0.0$ (i.e. $[(Mg_{1/3}Ta_{2/3})_{0.2}(Zn_{1/3}Ta_{2/3})_{0.8}]O_2$), both of the $MgTa_2O_6$ (trirutile structure, ICDD No. 32-631) and $ZnTa_2O_6$ (tri-αPbO_2 structure, ICDD No. 39-1484) patterns of roughly the same fractions were detected (i.e. $V_{T\alpha} \leqslant V_{Tr}$, where $V_{T\alpha}$ and V_{Tr} stand for the volume fractions of the tri-αPbO_2 and trirutile structures, respectively) by qualitative comparison of the peak intensities. At $x=0.2$, the trirutile structure preferentially decreased in intensity, whereas reflections of $MgNb_2O_6$ (columbite structure, ICDD No. 33-875) began to develop, resulting in the detection of mostly tri-αPbO_2 with small amounts of columbite and trirutile (i.e. $V_{Tr} \cdot V_C < V_{T\alpha}$, where V_C stands for the columbite fraction). At $x=0.4$, the columbite and trirutile structures coexisted ($V_{Tr} \cdot V_C$), while columbite was the sole structure identified at $x=0.6$ and 0.8 (i.e. $[(Mg_{1/3}Ta_{2/3})_{0.2}(Mg_{1/3}Nb_{2/3})_{0.8}]O_2$). Therefore, it was revealed that the $MgTa_2O_6$ component of 20 mol% (introduced to the $[(Zn_{1/3}Ta_{2/3}),(Mg_{1/3}Nb_{2/3})]O_2$ system) retained its own structural identity at low values of x, whereas assimilated structurally to the columbite at high values of x.

XRD results taken after the PbO addition and calcination procedures are presented in Fig. 2. At a PZT-rich composition of $x=0.0$ ($Pb[(Mg_{1/3}Ta_{2/3})_{0.2}(Zn_{1/3}Ta_{2/3})_{0.8}]O_3$), only a pyrochlore structure developed (similar to the case of a stoichiometric PZT composition [14]), along with small amounts of PbO and ZnO. The two oxides seem to be the components left after formation of the pyrochlore (Pb- and Zn-deficient as compared with a perovskite stoichiometry) from a mixture intended for the perovskite development. Such a reasoning is supported by the observation that the two oxides were detected only at compositions where the pyrochlore is the major structure. Meanwhile, the perovskite phase started to develop from $x=0.2$ and became predominant at $0.4 \leqslant x$.

Systematic shifts in the reflection angles with compositional change were scarcely observable (similar to the PZT–PMN system [14]), which is in accordance with the evidence [15–17] that ionic size of Ta is actually somewhat smaller than that of Nb, even though their sizes were reported identical (0.064 nm [18]). It is believed that the smaller size of Ta compensates for the larger Zn (0.0740 nm, as compared with 0.0720 nm of Mg [18]),

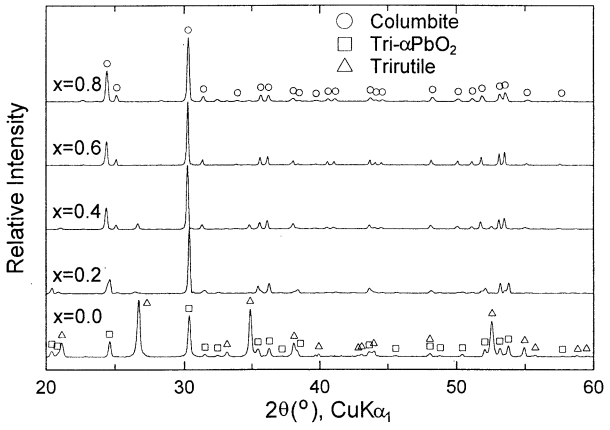

Fig. 1. X-ray diffraction results of the B-site precursor $[(Mg_{1/3}Ta_{2/3})_{0.2}(Zn_{1/3}Ta_{2/3})_{0.8-x}(Mg_{1/3}Nb_{2/3})_x]O_2$ system.

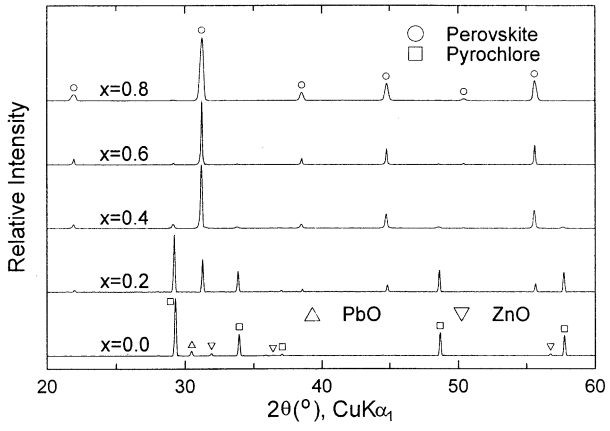

Fig. 2. X-ray diffraction results of the 0.2PMT–(0.8–x)PZT–xPMN system.

resulting in approximate balance between the effective sizes of the $Zn_{1/3}Ta_{2/3}$ and $Mg_{1/3}Nb_{2/3}$ octahedral–cation complexes. As a result, perovskite lattice parameters would not change appreciably. Meanwhile, extraneous reflections (associated with the perovskite superstructure) were not detected throughout the system, indicating an absence of any long-range ordering among the multiple-octahedral cations of 3–4 species.

Fig. 3 shows the perovskite development yields after each heat-treatment stage. As was observed in Fig. 2, the perovskite content was 0% (even after sintering) at $x=0.0$. The yield (after sintering) then increased to ~36% ($x=0.2$), ~95% ($x=0.4$), and 100% ($x=0.6$ and 0.8). The rapid increase at low values of x is definitely associated with the decreased fraction of PZT, perovskite development of which has not succeeded yet. Furthermore, the content also increased with heat treatments: e.g. ~29%, ~33%, and ~36% at $x=0.2$ after the first and second calcinations, and after the sintering, implying thermodynamic stability of the perovskite structure over the pyrochlore. Such increases in the perovskite yield could be well exploited in the further promotion of the perovskite formation, were it not for the inevitable PbO volatilization during prolonged exposure to high temperatures. Relative densities of the sintered samples were ~95% ($x=0.4$), ~96% ($x=0.6$), and ~97% ($x=0.8$), as calculated based upon the perovskite lattice parameters.

Temperature-dependent dielectric responses of $x=0.8$ (i.e. 0.2PMT–0.8PMN) are displayed in Fig. 4 as a function of measurement frequency. The spectra showed typical relaxor behavior of dielectric dispersion and diffuse modes in the phase transition. Maximum dielectric constant values were 15,000 (−25 °C), 14,000 (−20 °C), 12,900 (−15 °C), and 11,700 (−7 °C) at 1, 10 and 100 kHz, and 1 MHz, respectively, while maximum losses were 13% (−43 °C), 15% (−38 °C), 17% (−34 °C), and 23% (−27 °C) at the same frequency decades. Other compositions in the system (except for $x=0.0$, where perovskite content = 0%) also showed similar frequency-dependent dielectric dispersion, but with different magnitudes and temperatures of the dielectric constant and loss maxima.

Dielectric constant spectra (1 kHz) of the whole compositions in the system are compared in Fig. 5. An ever-decreasing trend in the dielectric constant was observed at $x=0.0$ (0.2PMT–0.8PZT, where only the pyrochlore structure developed), with room temperature value and temperature coefficient of 75 and -3.7×10^{-2}/K, respectively. With increasing x (i.e. PMN concentration), the maximum value increased tremendously from 580 ($x=0.2$) to 15,000 ($x=0.8$). In contrast, the dielectric maximum temperatures remained almost unchanged at −31 to −25 °C, approximately 20 °C lower than those of the PZT–PMN system [14]. The decreases in the

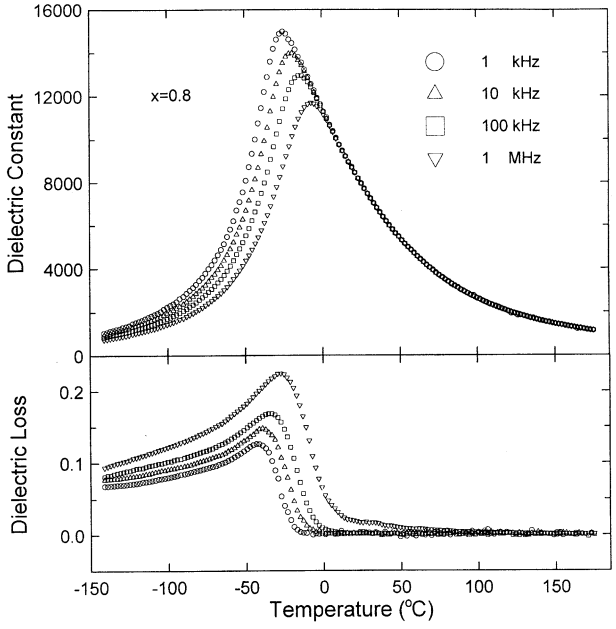

Fig. 4. Frequency-dependent dielectric constant and loss spectra of $x=0.8$.

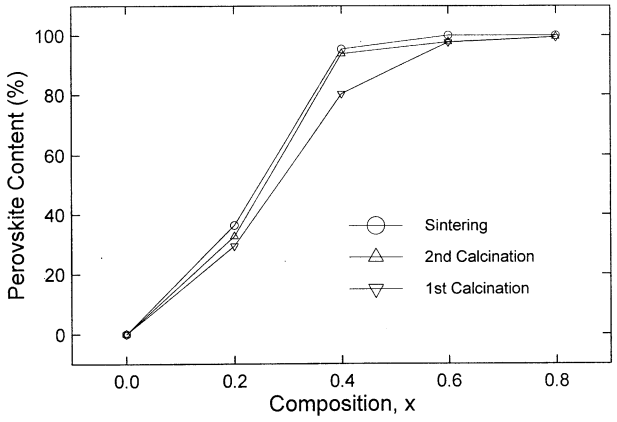

Fig. 3. Perovskite contents of the 0.2PMT–(0.8–x)PZT–xPMN system compositions.

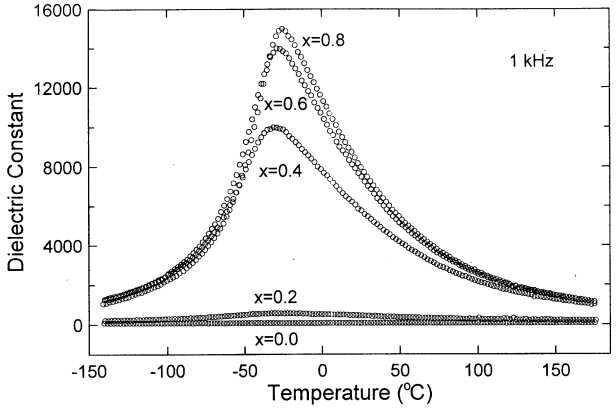

Fig. 5. Dielectric constant spectra of the entire system ceramics (1 kHz).

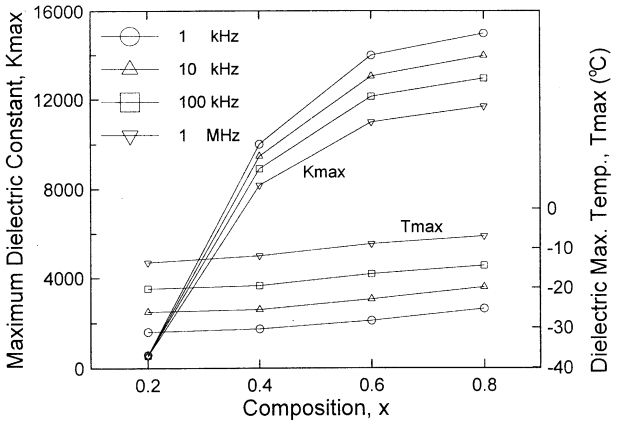

Fig. 6. Dependencies of the maximum dielectric constant and dielectric maximum temperature upon composition and measurement frequency.

dielectric maximum temperature are undoubtedly due to the introduction of PMT with a quite low dielectric maximum temperature of −87 to −85 °C [3–5].

Variations of the maximum dielectric constant (K_{max}) and dielectric maximum temperature (T_{max}) with changes in composition and frequency are replotted in Fig. 6. As observed in Fig. 5, K_{max} increased rapidly with increasing x, whereas T_{max} stayed nearly constant, regardless of measurement frequency. It is quite interesting to note that the dielectric maximum temperatures of such a wide range in composition are rather insensitive to the compositional change. Besides, degrees of the dielectric dispersion ($T_{max,1MHz}$–$T_{max,1kHz}$) were also nearly constant at 17–19 °C throughout the entire composition.

Phase transition modes reflected in the dielectric constant spectra are often analyzed with respect to diffuseness parameters of diffuseness exponent (γ) and degree of diffuseness (C/K_{max}), meanings and derivation methods of which can be found elsewhere [14,19–23]. Composition-dependent relations of $\log(1/K–1/K_{max})$ versus $\log(T–T_{max})$ are presented in Fig. 7, from which values of the two diffuseness parameters were obtained and are plotted in the inset. Values of the two parameters decreased only slightly from 1.71 to 1.66 and from 1170 to 650, respectively, with increasing x. The changes of the diffuseness parameters in the present system are rather small, compared with those in other systems [22–24].

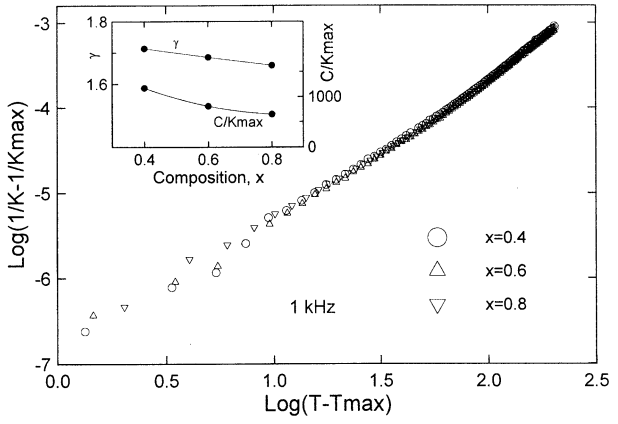

Fig. 7. $\log(1/K–1/K_{max})$ versus $\log(T–T_{max})$ of the 0.2PMT–(0.8–x)PZT–xPMN system. Variations of the diffuseness exponent (γ) and degree of diffuseness (C/K_{max}) with compositional change are separately shown in the inset.

4. Summary

Columbite, trirutile, and tri-αPbO_2 structures developed in the B-site precursor system. Columbite was stable at high values of x, whereas the other two structures were detected at the other end of the system. After PbO addition, perovskite and pyrochlore developed in the entire composition range, but the former structure was mostly detected at high values of x (i.e. PMN-rich compositions), whereas the latter was detected at low x of PZT-rich compositions. Consequently, the perovskite phase yield rose with increasing values of x at the expense of the pyrochlore.

Diffuse phase transition modes, with typical relaxor behavior, were observed at all compositions of the system (except for $x=0.0$). At $x=0.8$, the maximum dielectric constants and corresponding temperatures were 15,000 (−25 °C), 14,000 (−20 °C), 12,900 (−15 °C), and 11,700 (−7 °C) at 1, 10, and 100 kHz, and 1 MHz, respectively. Temperatures corresponding to the maximum loss also rose with increasing frequency, but the temperatures were 18–20 °C lower than the dielectric maximum temperatures. With decreasing x (i.e. increasing PZT concentration), magnitudes of the dielectric constant peak decreased remarkably from 15,000 ($x=0.8$) to 580 ($x=0.2$) at 1 kHz, while temperatures of the peak remained nearly constant (−31 to –25 °C). Analyses of the phase transition mode in terms of diffuseness revealed that dependencies of the two diffuseness parameters upon composition were only slight.

Acknowledgements

This study was supported by the Korea Research Foundation under grant KRF-99-041-E00528.

References

[1] S.L. Swartz, T.R. Shrout, Mater. Res. Bull. 17 (1982) 1245.
[2] B.-H. Lee, N.-K. Kim, J.-J. Kim, S.-H. Cho, Ferroelectrics 211 (1998) 233.
[3] Z.G. Lu, C. Flicoteaux, G. Calvarin, Mater. Res. Bull. 31 (1996) 445.
[4] M.A. Akbas, P.K. Davies, J. Mater. Res. 12 (1997) 2617.
[5] M.-C. Chae, N.-K. Kim, J.-J. Kim, S.-H. Cho, Ferroelectrics 211 (1998) 25.

[6] B.A. Malkov, Y.N. Venevtsev, Inorg. Mater. 13 (1977) 1189.
[7] M.A. Akbas, P.K. Davies, J. Am. Ceram. Soc. 80 (1997) 2933.
[8] P. Ravindranathan, V. Srikanth, S. Komarneni, A.S. Bhalla, Ferroelectrics 188 (1996) 135.
[9] J. Wang, D. Wan, J. Xue, W.B. Ng, J. Am. Ceram. Soc. 82 (1999) 477.
[10] S.-E. Park, M.L. Mulvihill, P.D. Lopath, M. Ziparro, T.R. Shrout, Proc. 10th IEEE ISAF, 1996, pp. 79–82.
[11] C.S. Park, K.Y. Lim, D.Y. Choi, S.J. Chung, J. Kor. Phys. Soc. 32 (suppl.) (1998) S974.
[12] T.R. Shrout, A. Halliyal, Am. Ceram. Soc. Bull. 66 (1987) 704.
[13] H.C. Ling, M.F. Yan, W.W. Rhodes, Ferroelectrics 89 (1989) 69.
[14] M.-C. Chae, S.-M. Lim, N.-K. Kim, Ferroelectrics 242 (2000) 25.
[15] A.V. Titov, O.I. Chechernikova, Y.N. Venevtsev, Inorg. Mater. 14 (1978) 891.
[16] C.G.F. Stenger, A.J. Burggraaf, Phys. Status Solidi (a) 61 (1980) 275.
[17] M.-C. Chae, N.-K. Kim, Ferroelectrics 209 (1998) 603.
[18] R.D. Shannon, Acta Cryst. A32 (1976) 751.
[19] S.-M. Lim, N.-K. Kim, J. Mater. Sci. 35 (2000) 4373.
[20] K. Uchino, S. Nomura, Ferroelectrics Lett. 44 (1982) 55.
[21] S.J. Butcher, N.W. Thomas, J. Phys. Chem. Solids 52 (1991) 595.
[22] M. Kuwabara, S. Takahashi, K. Goda, K. Oshima, K. Watanabe, Jpn, J. Appl. Phys 31 (9B) (1992) 3241.
[23] B.-Y. Ahn, N.-K. Kim, J. Am. Ceram. Soc. 83 (2000) 1720.
[24] J.-S. Kim, N.-K. Kim, Mater. Res. Bull. 35 (2000) 2479.